Microsc. Microanal. 8 (Suppl. 2), 2002
DOI 10.1017.S1431927602101073

Electron Microscopy Study Of Misfit Layer Structures In The Sb-Nb-S And Bi-Nb-S Systems

L. C. Otero-Díaz

Dpto. Quím. Inorgánica, F. CC. Químicas and CME, Univ. Complutense, E-28040, Madrid, Spain

The misfit layer chalcogenides constitute a broad group of minerals (as cylindrite, cannizzarite,...) and synthetic inorganic materials [1,2]. Their ideal stoichiometry is $(AX)_{1+\delta}(BX_2)_n$ (A=rare earth, Sn, Pb, Sb, Bi; B=Ti, V, Cr, Nb, Ta; X=S, Se) and they are built up by alternate stacking of two sub-structural units with their own underlying average lattices: (a) a so-called H sublattice, with pseudo-orthohexagonal symmetry, formed by n adjacent (BX_2) sandwiched three-atom-thick layers with a structure similar to the one found in the parent transition metal chalcogenide and; (b) a so called Q sublattice, with pseudo-tetragonal symmetry, formed by one (AX) two-atom-thick layer with a distorted rock-salt structure. (1+δ) is given by the interlayer misfit.

Samples with nominal composition ANb_2S_5 (A=Sb, Bi) were prepared from the elements [3,4]. Electron microscopy observations were performed in scanning (30 kV) and transmission (200 and 400 kV) microscopes. The SAEDP's taken along the main orientations have allowed us to characterize seven new misfit layer structures in both systems. So, figure 1 (a, b, c, and d) corresponds to the Fourier-filtered high resolution images and diffraction patterns of the monolayer $(SbS)_{1.195}NbS_2$ along the indicated directions. Note the modulations bands marked by arrows in a, and the stacking planes in c. Figure 2-a shows a SEM micrograph of an agglomerate of $(BiS)_{1.166}(NbS_2)_2$ misfit layer crystals. The SAEDP of one of these crystals, taken along [001], is shown in 2-b. The main reflections, marked with arrowheads, are indexed as 200_Q, 200_H and $020_{H,Q}$ (without labelling). The arrows indicate the modulation q vector (~0.4 nm period) that defines the misfit modulation. The small arrows denote and additional modulation, which seems to be beam sensitive. Thus in the figure 2-c the high resolution processed image contains only information coming from the primary modulation, see the arrows.
We have also observed big crystals (mm-sized) with variable tubular morphology (see the scanning micrograph given in figures 3-a,b). BSE imaging and WEDS analysis of single tubular crystals and TEM of their cross sections (Figures 3-c,d) revealed a strong compositional and inter-laminar stacking disorder along the tube radius. Slabs with stacking sequences corresponding to binary 3 R-NbS_2 (~0.6 nm) and $BiNb_2S_5$ (~1.74 nm) which dominate in the crystal have been found, see figure 3-e. Besides the disordered areas, a new related phase ~$BiNb_4S_9$ with a stacking sequence ..Q, H, H, H, H.. and ~2.92 nm periodicity was observed. In table 1 we present the crystal unit cell refined parameters for two phases, a monolayer ~$SbNbS_3$ (..Q,H..) and a bilayer ~$BiNbS_5$ (..Q,H,H..). Those values were obtained after the approximated ones were measured from the SAEDP's along the main orientations. The distortions of the Q and H subcells from ideal tetragonality and hexagonality, **b/a** values, are also included.

References

[1] E. Makovicky and B. G. Hyde, Mater. Sc. Forum 100-101 (1992) 1.
[2] G. A. Wiegers, Prog. Solid State Chem, 24 (1996) 1.
[3] L. C. Otero-Díaz et al, J. Solid State Chem, 115 (1995) 274.
[4] A. R. Landa-Cánovas et al, Micron 32 (2001) 481.
[5] This work was supported by the Spanish CYCIT project MAT2000-0753-C02-01. The help of Mr. Gómez-Herrero and Dr. Landa-Cánovas from Univ. Complutense is gratefully acknowledged.

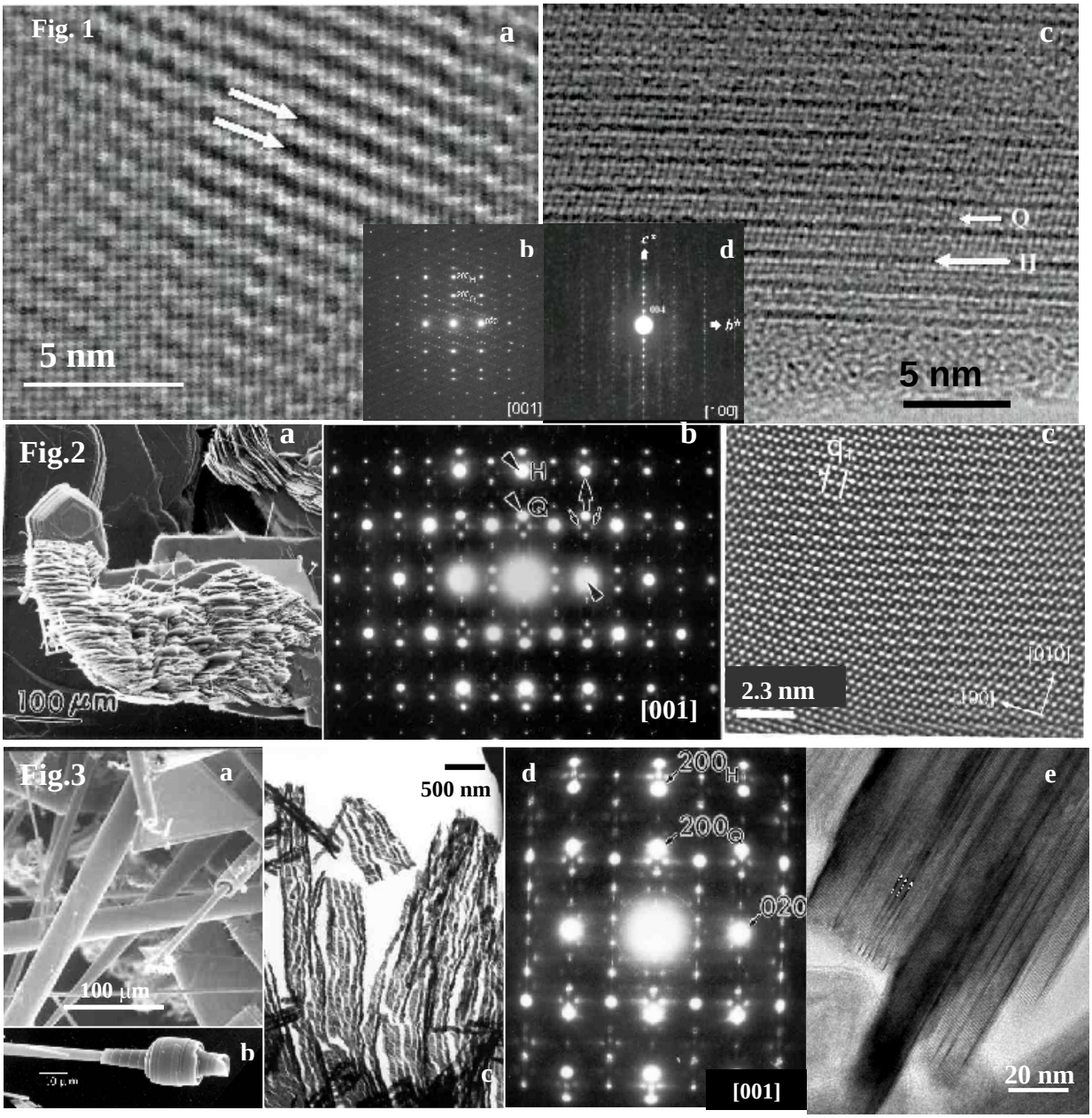

Table 1: Refined unit cell parameters from X-ray powder diffraction data.

Phase	**Subcell**	**a** (nm)	**b** (nm)	**c** (nm)	α (º)	β (º)	γ (º)	**b/a**
$(SbS)_{1.195}NbS_2$	Q (SbS)	0.5560(1)	0.5693(4)	2.2834(3)	90	90	90	1.024
	H (NbS_2)	0.3321(6)	0.5701(8)	1.1411(4)	90	90	90	1.717
$(BiS)_{1.166}(NbS_2)_2$	Q (BiS)	0.5682(2)	0.5769(1)	1.7416(5)	93.26(2)	90	90	1.015
	H (NbS_2)	0.3313(1)	0.5774(1)	1.7419(3)	93.15(2)	90	90	1.743

https://doi.org/10.1017/S1431927602101073 Published online by Cambridge University Press